Agricultural and Forest Meteorology 252 (2018) 10–17

Contents lists available at ScienceDirect

Agricultural and Forest Meteorology

journal homepage: www.elsevier.com/locate/agrformet

Vegetation can strongly regulate permafrost degradation at its southern edge through changing surface freeze-thaw processes

Weichao Guo[a], Hongyan Liu[a,*], Oleg A. Anenkhonov[b], Huailiang Shangguan[a], Denis V. Sandanov[b], Andrey Yu. Korolyuk[c], Guozheng Hu[a], Xiuchen Wu[d]

[a] College of Urban and Environmental Science, and MOE Laboratory for Earth Surface Processes, Peking University, Beijing, 100871, China
[b] Institute of General and Experimental Biology, Siberian Branch, Russian Academy of Sciences, Ulan Ude, 670047, Russia
[c] Central Siberian Botanical Garden, Siberian Branch, Russian Academy of Sciences, Novosibirsk, 630090, Russia
[d] Faculty of Geographical Sciences, Beijing Normal University, Beijing, 100875, China

ARTICLE INFO

Keywords:
Permafrost degradation
Freeze-thaw
Vegetation
Snow accumulation

ABSTRACT

Permafrost contains twice as much carbon as the atmosphere and the degradation of permafrost due to climatic warming, which could potentially change the global carbon cycle and could also enhance global climate change. It is well studied that permafrost degradation could result in vegetation transition. Aboveground vegetation can act as a buffer for climatic warming, however its role in regulating permafrost degradation remains unclear. In this study we examined how different vegetation types regulated the amplitude and duration of diurnal soil freeze/thaw (FT) cycles and the timing of seasonal soil FT. Soil temperature data (hourly and half hourly) was collected from paired forest-steppe sampling plots spanning a large spatial gradient from northern China to southern Siberia, Russia from 2008 to 2015. FT cycles were found to be larger in amplitude and longer in duration in steppe sites in comparison to forest sites. Soils in the forest sites and steppe sites freeze almost simultaneously, but experience a delay in thawing of approximately 14, 19 and 25 days for deciduous broadleaf forest, evergreen coniferous forest, and deciduous coniferous forest, respectively. Variations in snow accumulation due to differences in vegetation structure as opposed to solar radiation were responsible for the disparity in thaw timing. These findings imply that deciduous conifer forest in east Eurasia could reduce carbon emissions more effectively than evergreen conifer forest in west Eurasia by slowing down warming-induced permafrost degradation during spring thaw.

1. Introduction

Permafrost (permanently frozen ground) comprises a region underlying 23.9% of the land area of the Northern Hemisphere. Currently permafrost contains about twice as much carbon as the atmosphere (Zhang et al., 1999; Zimov et al., 2006). These large quantities of carbon stored in frozen soils can be released into the atmosphere due to warming-induced permafrost degradation, which is further enhanced by a warming climate (Hodgkins et al., 2014; Hollesen et al., 2015; Schuur et al., 2015). This degradation could cause permafrost regions to shift from being a sink to a source of CO_2 by the end of the 21st century (Koven et al., 2011). Permafrost degradation mainly occurs at the southern edge of the permafrost area due to the significant poleward movement of permafrost with climate warming (Guo and Wang, 2016). Soil freezing–thawing (FT) processes are measured by the amplitude and duration of the diurnal soil FT cycle as well as seasonal FT timing and can effectively mediate permafrost degradation. Increasing soil surface thawing days can enhance permafrost degradation by deepening active layer thickness (Peng et al., 2017; Wu et al., 2015; Zhang, 2005). The soil suffers remarkable FT cycles during the transition period from cold/warm to warm/cold seasons. The transition between frozen soil to thawing is a continuous process lasting from several days to a few weeks (Cheng et al., 2014; Wang et al., 2013), and is susceptible to rapid climate warming, in particular the higher warming rates that occur in winter and spring (IPCC, 2013). Stronger and longer diurnal FT cycles and earlier seasonal permafrost thawing may increase carbon loss from the soil.

There has been significant research examining spatio-temporal changes in soil FT processes in response to a warming climate at regional and continental scales, mainly using land surface temperature data from satellites (Kim et al., 2014; Li et al., 2012; Zhang, 2003) and land surface model simulations (Guo and Wang, 2014). Despite this, uncertainties still exist in the conclusions of these studies due to the coarse resolution of the available data and poor representation and

* Corresponding author.
E-mail address: lhy@urban.pku.edu.cn (H. Liu).

https://doi.org/10.1016/j.agrformet.2018.01.010
Received 20 July 2017; Received in revised form 25 November 2017; Accepted 5 January 2018
Available online 10 January 2018
0168-1923/ © 2018 Elsevier B.V. All rights reserved.

parameterization of soil FT processes. To comprehensively understand soil FT processes at a regional scale, long-term direct monitoring of these processes in the field over a large spatial and climactic gradient is needed (Cheng et al., 2014; Sun et al., 2012). However, this is currently rare, preventing a detailed understanding of patterns and drivers of soil FT processes.

Long-term climate warming could disequilibrium the relationship between vegetation and permafrost (Camill and Clark, 1998). Most previous studies have focused on how permafrost degradation affect biomass and aboveground net primary production (Camill et al., 2001), vegetation recruitment (Camill et al., 2010), and vegetation fragmentation (Baltzer et al., 2014). Also, there are some researches concerning the vegetation impact on permafrost degradation. Field measurements in interior Alaska (Jorgenson et al., 2010), Jubany (King George Island) and Signy Island in the Maritime Antarctic (Cannone et al., 2006) found that vegetation could exert negative effect on permafrost degradation. However, a significant knowledge gap remains in terms of the regulative role of vegetation in permafrost degradation over a regional scale and long-term direct monitoring of soil temperature as proxy, especially by soil FT processes underground. Different vegetation types have distinct community structures, and consequently differ in solar radiation income, litter cover and snow accumulation patterns. Increasing LAI (leaf area index) could increase vegetation canopy and then raise the interception of snow which could affect snow accumulation in the interior of vegetation during the winter period (Pomeroy et al., 2002; Rasmus et al., 2011). Different snow accumulations could produce various influences on soil temperature variations (Iwata et al., 2010; Park et al., 2014b). These differences can substantially affect the energy balance within the soil-vegetation-atmosphere system and the thermal dynamics of the soil. We thus hypothesize that vegetation type can significantly influence diurnal soil FT cycles and the timing of seasonal soil FT.

Eleven paired forest-steppe measurement sites were located along a vast latitudinal (> 10°) and longitudinal (> 30°) gradient on the edge of the permafrost region of southern Siberia, Russia and northeastern China where permafrost degradation is more sensitive than in Canada and the USA (Guo and Wang, 2016). Soil FT processes were recorded directly and continuously at these sites from 2008 to 2015 (Fig. 1). Using the soil temperature observations collected during this eight year period, this study investigated the effects of vegetation type on the duration and amplitude of diurnal FT cycles and the timing of seasonal soil FT (see Materials and Methods).

2. Materials and methods

2.1. Study region

Our study region is located in southern edge of a permafrost region in Inner Mongolia, China and southern Siberia, Russia (Fig. 1). This region is predominantly covered by forest-steppe transitional vegetation, with forests distributed mainly on shady slopes and steppes found on sunny slopes and flatlands (Gutiérrez-Jurado et al., 2013; Hu et al., 2013; Namzalov et al., 2012). The mean annual temperature ranges from −4.5 °C in the north to 3.5 °C in the south of this region, and mean annual precipitation ranges from 350-550 mm (Table S1). We established four sampling sites in the Altai Mountains, three sampling sites in the Trans-Baikal region of Russia and four sampling sites on the eastern Inner Mongolian Plateau in China (Fig. 1).

2.2. Vegetation types

In each site, we selected two typical aspect-dependent vegetation plots. One was located in forest and the other was in the adjacent steppe. These paired plots were several hundred meters apart. Forest sample plots were either dominated by *Larix sibirica* (larch), *Pinus sylvestris* (pine) or *Betula platyphylla* (birch). These species belong to different vegetation types, deciduous conifer, evergreen conifer and deciduous broadleaf forest, respectively and their morphological and ecophysiological features differ from each other. While *L. sibirica* and *P. sylvestris* are both conifers, *P. sylvestris* is evergreen and can intercept some snow in the canopy layer, decreasing its penetration to the forest interior, however the deciduous *L. sibirica* cannot.

2.3. Soil temperature measurements

We placed temperature data loggers (HOBO, Onset Computer Corporation, MA, USA) into about 10 cm in depth below ground surface, and logged soil temperature hourly or half hourly. Data loggers were set in the interior of the sample plots, without depression and root around. Loggers were installed in the soil in 2008, with the exception of the Altai Mountains, where loggers were not installed until 2010. The data was downloaded from the loggers during the transition from summer to autumn of each year and the battery was also checked, and if necessary replaced, before replacing the logger into the soil.

Total potential solar radiation (TPSR). TPSR were calculated by using Solar Calculator tool (http://www.meteoexploration.com/products/SolarCalculator.html). While giving the specific location (latitude and longitude), timing, altitude, temperature, etc (Table S1), we calculated the TPSR for each forest-steppe sample plots.

2.4. Soil temperature, precipitation and solar radiation of USCRN (the U.S. climate reference network)

USCRN is a network of meteorological stations maintained by the National Oceanic and Atmospheric Administration which have been measuring soil temperatures since 2011 (Bell et al., 2013). In order to explore the impact of snow depth and solar radiation on soil thaw timing with different vegetation types, USCRN is prior to this research which contains soil temperature, precipitation and solar radiation and could help us to build connection between vegetation types and soil thaw timing. It appears that precipitation during freezing time is a proxy for snow accumulation.

2.5. Estimation of soil freeze/thaw parameters

Difference in Julian day of year (DOY) was used to compare the difference in soil thawing and freezing dates between paired forest-steppe samples for different vegetation types. New Year's Day is defined as DOY 1, and the last day of the year is DOY 365 or 366 in a leap year. Soil temperature was used to determine periods of soil thawing and freezing. When daily minimum soil temperature exceeded 0 °C, it was categorized as a soil thawing day and when daily maximum soil temperature was below 0 °C, it was categorized as a soil freezing day.

When the daily maximum soil temperature exceeded 0 °C and the minimum soil temperature was below 0 °C in one day, this implies that the soil thawed during the day and froze again during the night, producing a FT cycle. We then calculated both the duration and amplitude of diurnal soil FT cycles during the soil freezing–thawing transitional periods. Duration of diurnal soil FT cycles was calculated using the number of days with diurnal soil FT cycles (Bartsch et al., 2007; Guo and Wang, 2014; Han et al., 2010). Duration was calculated for both freeze-to-thaw and thaw-to-freeze stages for each of the paired sample plots. Amplitude of diurnal soil FT cycles was evaluated using diurnal temperature ranges (difference between maximum and minimum soil temperature) for periods when diurnal soil FT cycles occurred (Henry, 2007).

3. Results

3.1. Diurnal soil FT cycles of different vegetation types

Comparisons of temperature variations within diurnal soil FT cycles

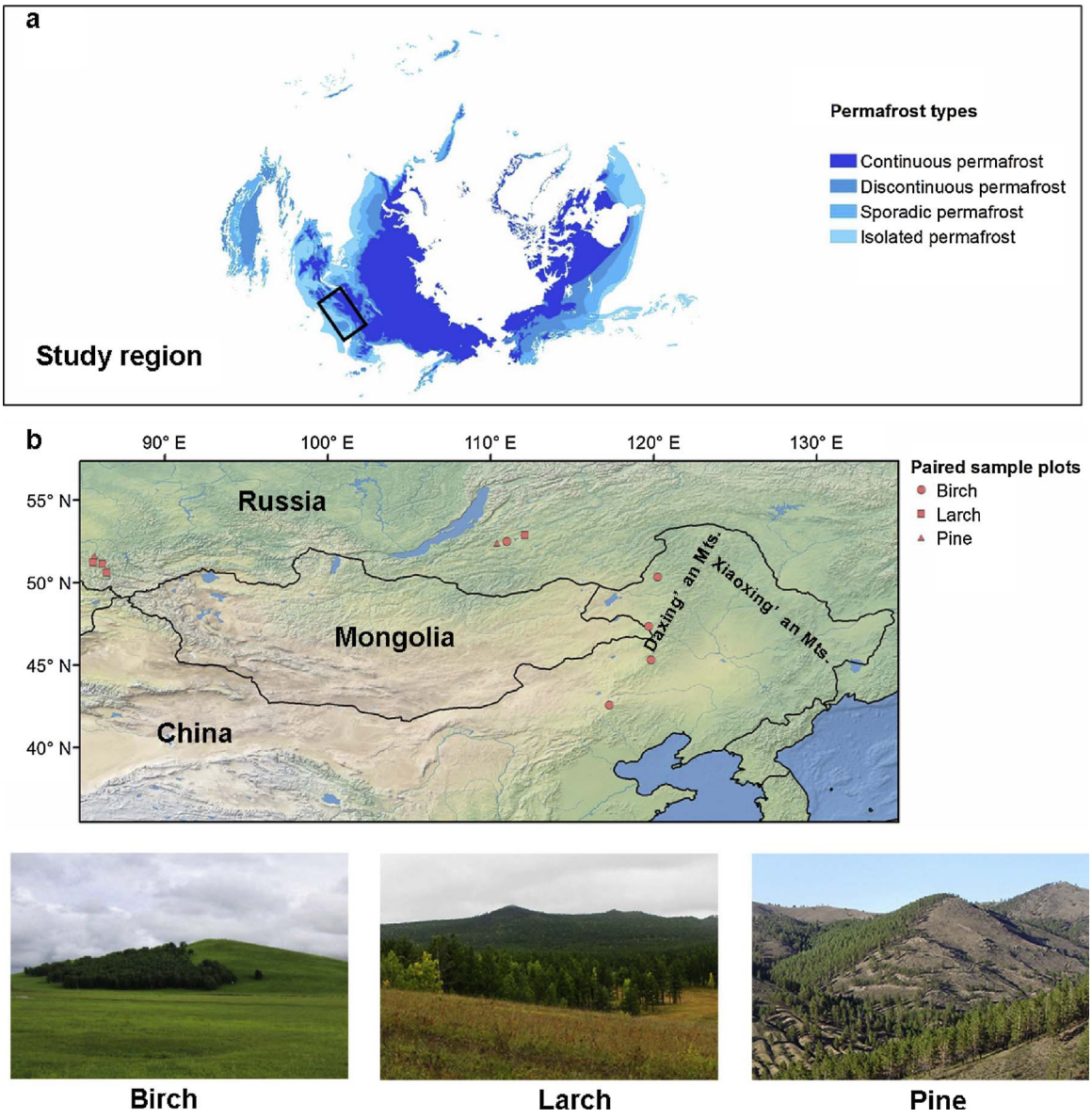

Fig. 1. Permafrost regions and study sites. Data from the IPA (International Permafrost Association) map showing present-day permafrost regions (a). Spatial distribution of paired forest-steppe sampling plots and landscape of three correspondingly dominant tree species in northern China and southern Siberia (b).

between paired forest and steppe sites show great difference during both soil thawing (Fig. S1a) and freezing periods (Fig. S1b). The detailed mean soil temperature variation, duration and amplitude of soil diurnal FT cycles are showed in Fig. S2, Table S2 and Table S3. The duration and amplitude (temperature ranges) of diurnal soil FT cycles are longer and larger in steppe plots than paired forest plots, which is validated by the PDF (Probability Distribution Function) of duration and amplitude of diurnal soil FT cycles between paired forest and steppe plots (Fig. S1c and S1d). The PDF of duration of diurnal soil FT cycles shows that steppe has approximately 10 days with diurnal soil FT cycles before they finally freeze or thaw. The duration of diurnal soil FT cycles in forests centralizes around 5 days (Fig. S1c). We also find that the maximum duration of FT cycles in steppe can last almost 60 days. Amplitude of diurnal soil FT cycles shows great difference between steppe and forest (Fig. S1d). Majority of amplitude of diurnal soil FT cycles among forest plots is much narrower and centralizes 1 °C. However, it shows great variations in steppe and the amplitude of diurnal soil FT cycles can even reach almost 30 °C. The PDF of duration and amplitude of diurnal soil FT cycles for forests and steppes shows similar pattern between freeze-to-thaw and thaw-to-freeze stages (Fig. S1e and S1f). The duration of diurnal soil FT cycles in thaw-to-freeze period is shorter than that in freeze-to-thaw stage (Fig. S1e). This result indicates that difference in temperature dynamic (duration and amplitude) of soil diurnal FT cycles in vegetation groups is much obvious than that in stage groups.

There is a distinct pattern in the distribution of duration-amplitude of diurnal soil FT cycles among forest and steppe plots despite great variations (Fig. 2). Furthermore, there also shows various differences according to three different vegetation types both in forest and steppe sites. Soils under pine sites have longer duration and larger amplitude of diurnal soil FT cycles than under larch and birch sites while steppe shows almost the same pattern for the three forest types.

3.2. Seasonal soil freezing/thawing timing

During the thaw-to-freeze transitional period, soils freeze at approximately the same time ($p > 0.05$) in the paired steppe and forest plots of different forest types, with the exception of birch forest (Fig. 3a–d). For all paired samples, soil froze on DOY (difference in Julian day of year; see materials and methods) 306 ± 10 in steppe sites

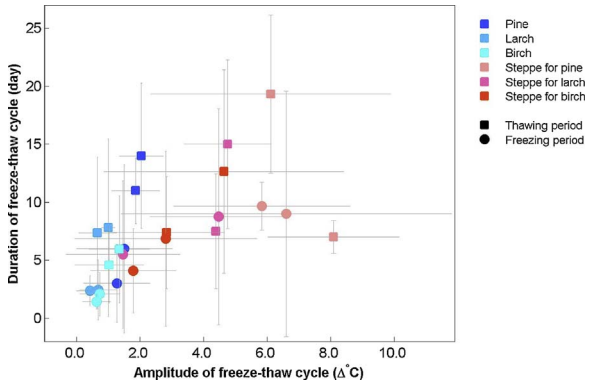

Fig. 2. Duration and amplitude of diurnal soil FT cycle for different vegetation types. Pine, larch and birch forest, and corresponding steppe sample plots are indicated using different colors. Square symbols represent data from the thawing period and circular symbols represent data from the freezing period. Horizontal and vertical gray lines represent standard deviations.

and DOY 304 ± 12 in forest sites (Fig. 3a). Soil in birch forests froze approximately 3 days earlier than the adjacent steppes ($p < 0.05$). The difference in freezing dates for paired forest-steppe samples in pine and larch forests was within 1–3 days (Table S4).

In contrast, there was a large difference in the timing of thawing between steppe and forest soils during the freeze-to-thaw transitional period in our study region for different forest types (Fig. 3e–h). For all sites, forest soils generally thawed on DOY 117 ± 12, approximately 17 days later ($p < 0.01$) than steppe soils (DOY 100 ± 12) in our study region (Fig. 3e). This confirms previous results, which were based on 3 years of observations (Hu et al., 2013) and illustrates the differences in the timing of thawing between paired forest-steppe samples for different forest types (Fig. 3f–h). The largest difference in the timing of thawing was observed in the paired forest-steppe samples in larch forests (Fig. 3g), where the forest soil thawed approximately 25 days later ($p < 0.01$) in larch compared with steppe soils (Fig. 3g). The soil in pine forests thawed approximately 19 days later than the paired steppe soils (Fig. 3f). The smallest difference was observed in the paired birch forest and steppe sites, with birch forest soils thawing approximately 14 days later than steppe (Fig. 3h).

Reanalysis based on the results from researches in Daxing'an Mountains/Xiaoxing'an Mountains, northeastern China showed that different forest types had various snow interception percentage. It ranges from 27.36 ± 4.15% in evergreen coniferous forest, 12.01 ± 3.51% in deciduous coniferous forest and 6.02 ± 4.05% in deciduous broadleaf forest (Fig. 4a). The onset of soil thawing in relation to climate shows that the timing of soil thaw was delayed by an

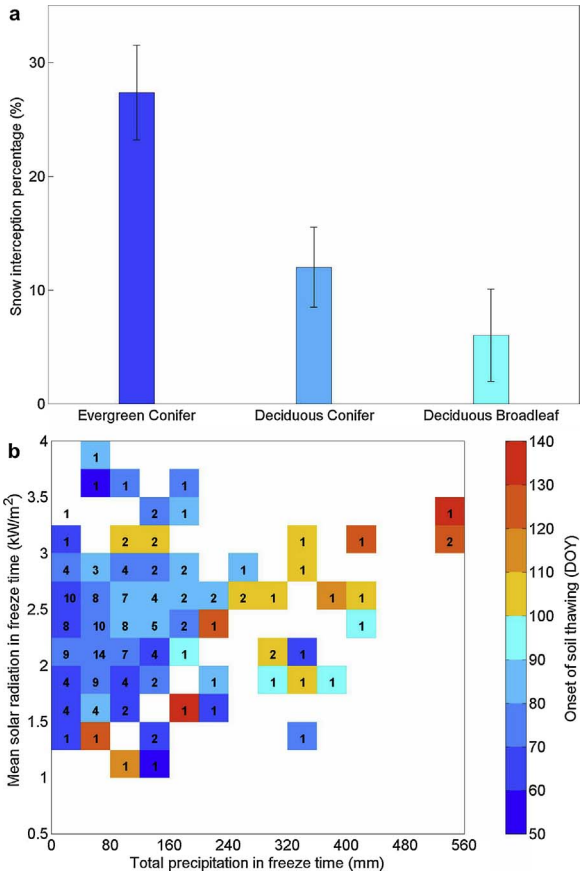

Fig. 4. Snow interception and onset of soil thawing in climate phrase space. Snow interception percentage for different vegetation types (a) are based on results from Table S5. Values for onset of soil thawing in climate phrase space (b) represents the amounts of FT processes.

increase in winter precipitation (a proxy for snow accumulation), and was not consistent with changes in solar radiation (Fig. 4b). Non-linear regression between the day of soil thaw onset and precipitation during freeze periods revealed a strong relationship between these factors ($R^2 = 0.25$; Fig. S3a). This also provides an explanation for the uncorrelated relationship between soil thaw and solar radiation (Fig. S3b).

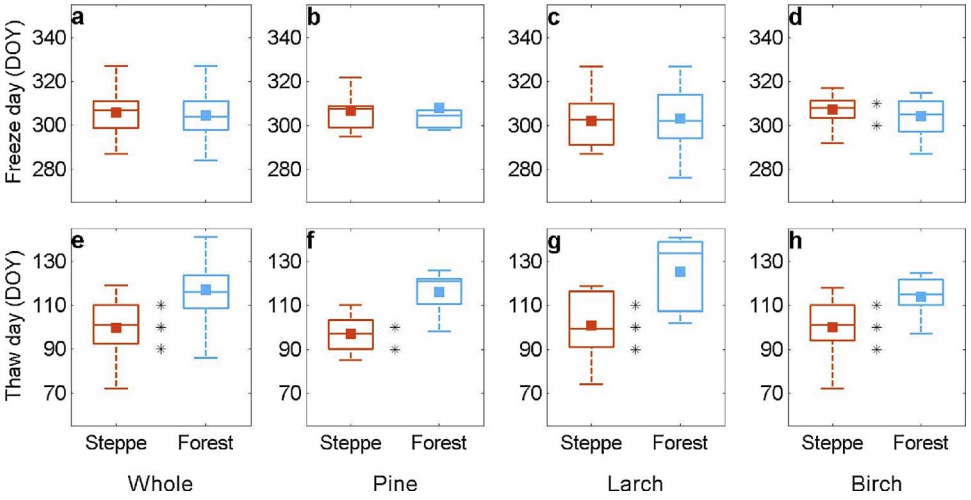

Fig. 3. DOY of soil thawing and freezing for the four vegetation types. Orange boxes represent steppe plots and blue boxes represent forest plots. DOY of soil freezing for all forest types in comparison to steppe sites are represented in (a), pine and steppe sites in (b), larch and steppe sites in (c) and birch and steppe sites in (d). Likewise DOY of soil thawing for all forest types in comparison to steppe sites are represented in (e), pine and steppe sites in (f), larch and steppe sites in (g) and birch and steppe sites in (h). Box plots show represent the mean (square), median (middle line), 25% (bottom of box), 75% (top of box), maximum (top of bar) and minimum (bottom of bar) DOY. Significance levels of paired t-tests are shown in the sub-figures. Two stars represent $p <= 0.05$, three stars represent $p <= 0.01$ and no star represents $p > 0.05$.

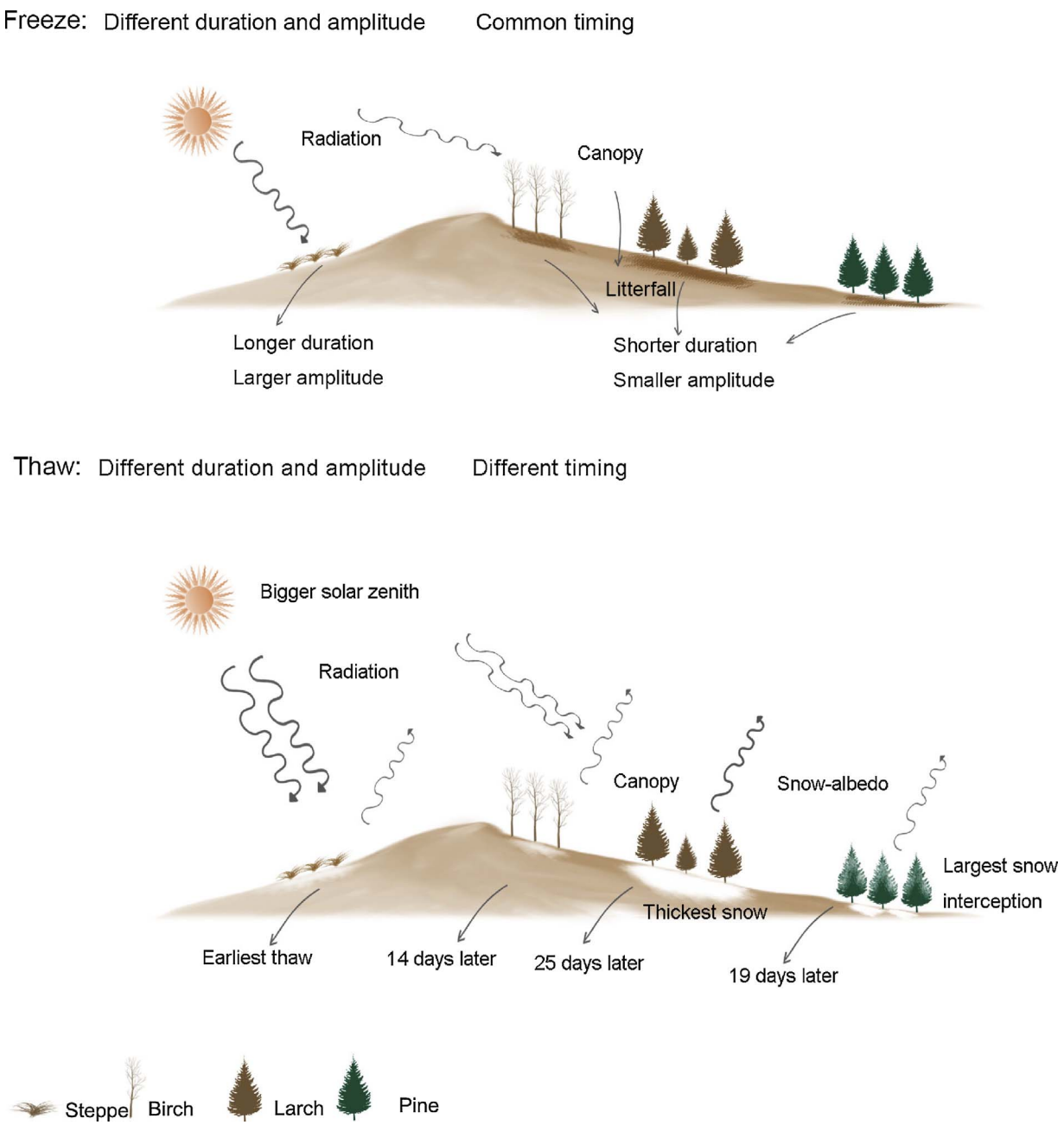

Fig. 5. Conceptualized diagram of the underlying mechanisms controlling soil freeze-thaw processes in steppe and three different forest types.

4. Discussion

4.1. Vegetation types not slope aspect mainly affected soil FT cycles

Slope aspect, coupled with vegetation type, plays an important role in producing differences in FT cycles (duration and amplitude). In the forest-steppe ecotone, areas of steppe vegetation are always on the sunny slope, while forest vegetation is found on shady slopes (Gutiérrez-Jurado et al., 2013). This type of landscape pattern is called "exposure-related forest-steppe" (Hais et al., 2016). Shady slopes receive less energy than sunny slopes (Berman et al., 2001) and the canopy and shoot of forest vegetation intercepts some sunlight, preventing it from reaching the forest floor (Binkley et al., 2010; Nelson et al., 2016; Smolander and Stenberg, 2001). Also, shady slope and canopy interception led to more shade which may limit decomposition in forest than steppe sites (Kochy and Wilson, 1997). This provides thermal insulation and has a buffering effect on soil temperature volatility within forested habitats.

Soil in the steppe sites is able to absorb more solar radiation than that in forest sites (Fig. S4). This is consistent with the finding that soil FT cycles were larger in amplitude and were longer in duration in steppe sites in comparison to adjacent forest sites. However, relationships between FT cycles (amplitude and duration) and TPSR (total potential solar radiation) were not found to be significant in either steppe or forest sites (Fig. S5). Radiation increased distinctly during the thawing period in comparison to the freezing period, but there was little change in the FT cycle for either forest or steppe sites. Therefore, different radiation due to slope aspect was not the main factor responsible for differences in amplitude and duration, which may be accounted for by vegetation structure. Another work across boreal ecosystems in central Alaska also proved that slope aspect was minor effects in permafrost degradation compared to vegetation types (Jorgenson et al., 2010). Canopy interception and litter insulation was higher in forest sites, producing a lower amplitude and shorter duration

of FT cycles in comparison with steppe sites.

4.2. Vegetation types mediated snow effects on seasonal soil freezing/thawing timing

The biggest difference between the soil thawing and freezing stages was the occurrence of snow cover, given that the vegetation canopy is almost equal between the two stages (before leaf growth and after leaf fall). Snow cover had not formed at the start of soil freezing, but snow accumulation during winter and early spring plays an important role in controlling the thermal transmission between the atmosphere and the soil during the soil thawing stage (Wu et al., 2016), due to albedo effects and snow effects on soil thermal insulation. Snow accumulation could have opposite effects on soil thaw, either enhancing soil thaw through increasing soil temperature (Iwata et al., 2010; Park et al., 2014a; Park et al., 2014b), or weakening soil thaw at its starting as suggested by our study. A study based on observed data and nine land surface models found that snow could insulate the soil from the cold air and warm soil temperature in the winter (Wang et al., 2016), however, its temperature was still below 0 °C and soil FT status did not change for most periods. In addition, differences in warming rates were larger than cooling rates between forest and steppe sites (Fig. S6). These suggested that the negative effect of snow on soil thaw might be larger than its positive effect, and consequently slow down soil thaw. Solar zenith is much higher during the thawing period than the freezing period, producing increased solar radiation during thawing (Fig. S4). Increased solar radiation income produces greater FT cycles (Fig. S1e and 1f), however, the absolute value of soil warming rate in most of the forest sample plots were lower than that of the cooling rate (Fig. S6). Snow-depth-dependent insulation buffered soil temperature variations in forest sites (Schindlbacher et al., 2014; Wang et al., 2013).

Snow accumulation was closely correlated with the canopy characteristics of trees (Hagedorn et al., 2014; Pomeroy et al., 2002; Rasmus et al., 2011). Our results showed that coniferous forest had a higher percentage of snow interception than broad-leaved forest. Therefore, less snow reached the interior of coniferous forest in comparison to a broad-leaved one (Lundberg et al., 2004). As pine forests are evergreen, the trees retained their leaves during winter. This caused the interception sublimation fraction of snow in the pine forest to be the highest among all four vegetation types (Lundberg et al., 2004), giving it a lower level of snow reservation than the larch forest. In addition, direct solar radiation and wind disturbance could contribute to the lowest level of snow accumulation in steppe sites in comparison with adjacent forest sites. Birch forest plots were located at the southernmost part of this permafrost region, which experiences less precipitation (Table S1), higher evaporation induced by higher winter temperatures and potentially has lower snow accumulation than coniferous forest plots (Gouttevin et al., 2012).

We suggest a conceptual model to explain the differences in soil FT dynamics among vegetation types during different stages, and the regulatory effects of different vegetation types (Fig. 5). Feedback of environmental factors (canopy structure, snow and solar radiation) and the soil FT processes (duration and amplitude of diurnal soil FT cycles and seasonal soil FT timing) were sufficiently different between steppe and the three corresponding forest types. Duration was longer and amplitude was greater for diurnal soil FT cycles in steppe sites during soil freezing and thawing periods. The largest differences were caused by vegetation structure and litter fall, not solar radiation from different slope aspects. Similarly, snow accumulation as opposed to solar radiation led to a delay in seasonal soil thawing in forest sites as opposed to steppe sites, in addition to differences among forest types.

4.3. Implications for future permafrost degradation

Climate projections show consistent permafrost degradation, which differ in extent according to different scenarios in a warmer future (Lawrence et al., 2012; Slater and Lawrence, 2013). ALT (active layer thickness) can reflect permafrost degradation which can be calculated from surface ATI (annual thaw index, the cumulative number of degree-days above 0 °C over a year) (Nelson and Outcalt, 1987). They show positive relationships with each other. Delay in thawing for three different forest sites could reduce ATI which can decrease ALT and permafrost degradation. A wide variety of up-to-date researches used Nelson's result and equation (Stefan solution) explore permafrost degradation and surface temperature (Peng et al., 2017; Wu et al., 2015). Furthermore, a study based on snow-vegetation-permafrost interaction found that snow accumulations among different alpine meadow covers could alter surface and deep-layer soil temperature dynamics, which affected active layer thickness (Chang et al., 2014). Overall, the observed weaker amplitude and shorter duration of diurnal soil FT cycles in the forest compared to the steppe sites implies that forest soil is more resistant to permafrost degradation than steppe soil. This is consistent with results from the Qinghai–Tibetan Plateau, which is mainly covered by alpine desert, steppe and meadow, which showed that active layer thickness increased more drastically here than other permafrost regions based on observations from 230 sites between 1990 and 2015 (Luo et al., 2016). In addition, the Qinghai–Tibetan Plateau permafrost may thaw faster than other permafrost regions in the future based on multimodel and multiscenario data from CMIP5 (the fifth phase of the Coupled Model Intercomparison Project) (Guo and Wang et al., 2016). These differences in thawing speeds can be explained by different sensitivities to rising air temperatures. The results from the present study provide additional data from the perspective of different vegetation types.

Permafrost contains about 50% of global soil stored carbon (Tarnocai et al., 2009). Current climate warming could lead to soil thaw in permafrost regions resulting in a loss of soil carbon in the form of methane and carbon dioxide emissions. Furthermore, asymmetric climate warming, with a higher warming rate in winter and spring (IPCC, 2013; Lawrimore et al., 2011), can significantly affect diurnal soil FT cycles in permafrost regions. Ongoing climate warming has raised global soil temperatures, especially in the northern hemisphere (Grillakis et al., 2016). This warming will exacerbate soil daily temperature dynamics (Brown and DeGaetano, 2011). It ultimately affect diurnal soil FT dynamics, particularly at permafrost edge regions which are more sensitive to climate change than inner regions (Guo and Wang, 2016). Forest vegetation could slow down permafrost degradation caused by climate warming, potentially decreasing carbon emissions (Baltzer et al., 2014; Blok et al., 2010).

In a warmer future, for example SRES A2 scenarios in CMIP3 models or RCP 8.5 scenarios in CMIP5 models, mean relative precipitation in winter is predicted to increase over permafrost regions (Knutti and Sedláček, 2012). As opposed to mixed forests found in North America, eastern Eurasian permafrost regions are dominated by deciduous needleleaf forest and western Eurasia is covered by evergreen needleleaf forest (Bartalev et al., 2003). Therefore, the soil in eastern Eurasia could experience a longer delay in thawing than that in western Eurasia where precipitation is predicted to increase in the future. Forests in the eastern Eurasian permafrost region could reduce soil thaw and carbon emissions more effectively than those in western Eurasia during spring thaw in response to a projected warmer climate.

In summary, our study reports a sufficiently different pattern in the diurnal soil FT processes between forest and steppe and further identifies the regulation effects of vegetation types/structures. We found that FT cycles were larger in amplitude and longer in duration in steppe sites compared to forest sites. Vegetation types not slope aspects played a major role in these paired forest-steppe observations. Soils in the forest sites froze almost simultaneously with steppe sites, but experience a delay in thawing of approximately 14–25 days for three different forest sites, attributed mainly to discrepancies in snow accumulation due to differences in vegetation structure as opposed to solar radiation. Asymmetric climate warming with a higher warming rate in spring

could speedup permafrost degradation, and deciduous conifer forest which widely distributed in east Eurasia could slow down permafrost degradation more effectively than evergreen conifer forest which widely distributed in west Eurasia.

Conflicts of interests

The authors declare that there are no conflicts of interest.

Acknowledgements

This study was supported by grants from National Natural Science Foundation of China (NSFC 41530747, 41325002, 41011120251, 41311120072, 41571038) and Russian Foundation of Basic Research (RFBR 13-04-91180, 10-04-91159, 16-54-53057). In addition, the research was carried out, in part, using the framework of projects supported by Russian Federal Budget, i.e. VI.52.1.9 to Oleg A. Anenkhonov and Denis V. Sandanov, and VI.52.1.4 to Andrey Yu. Korolyuk.

Appendix A. Supplementary data

Supplementary material related to this article can be found, in the online version, at doi:https://doi.org/10.1016/j.agrformet.2018.01.010.

References

Baltzer, J.L., Veness, T., Chasmer, L.E., Sniderhan, A.E., Quinton, W.L., 2014. Forests on thawing permafrost: fragmentation, edge effects, and net forest loss. Global Change Biol. 20 (3), 824–834.
Bartalev, S.A., Belward, A.S., Erchov, D.V., Isaev, A.S., 2003. A new SPOT4-VEGETATION derived land cover map of Northern Eurasia. Int. J. Remote Sens. 24 (9), 1977–1982.
Bartsch, A., Kidd, R.A., Wagner, W., Bartalis, Z., 2007. Temporal and spatial variability of the beginning and end of daily spring freeze/thaw cycles derived from scatterometer data. Remote Sens. Environ. 106 (3), 360–374.
Bell, J.E., et al., 2013. U.S. climate reference network soil moisture and temperature observations. J. Hydrometeorol. 14 (3), 977–988.
Berman, D., Alfimov, A., Mazhitova, G., Grishkan, I., Yurtsev, B., 2001. Cold Steppe in North-Eastern Asia. Magadan, Institute of Biological Problems of the North, Far-Eastern Branch of the Russian Academy of Sciences. pp. 1–183.
Binkley, D., Stape, J.L., Bauerle, W.L., Ryan, M.G., 2010. Explaining growth of individual trees: light interception and efficiency of light use by eucalyptus at four sites in Brazil. For. Ecol. Manage. 259 (9), 1704–1713.
Blok, D., et al., 2010. Shrub expansion may reduce summer permafrost thaw in Siberian tundra. Global Change Biol. 16 (4), 1296–1305.
Brown, P.J., DeGaetano, A.T., 2011. A paradox of cooling winter soil surface temperatures in a warming northeastern United States. Agric. For. Meteorol. 151 (7), 947–956.
Camill, P., et al., 2010. Early life history transitions and recruitment of Picea mariana in thawed boreal permafrost peatlands. Ecology 91 (2), 448–459.
Camill, P., Clark, J.S., 1998. Climate change disequilibrium of Boreal Permafrost Peatlands caused by local processes. Am. Nat. 151 (3), 207–222.
Camill, P., Lynch, J.A., Clark, J.S., Adams, J.B., Jordan, B., 2001. Changes in biomass, aboveground net primary production, and peat accumulation following permafrost thaw in the Boreal Peatlands of Manitoba, Canada. Ecosystems 4 (5), 461–478.
Cannone, N., Ellis Evans, J.C., Strachan, R., Guglielmin, M., 2006. Interactions between climate, vegetation and the active layer in soils at two Maritime Antarctic sites. Antarct. Sci. (03), 18.
Chang, J., Wang, G.-x, Gao, Y.-h, Wang, Y.-b., 2014. The influence of seasonal snow on soil thermal and water dynamics under different vegetation covers in a permafrost region. J. Mt. Sci. 11 (3), 727–745.
Cheng, Q., et al., 2014. In situ measured and simulated seasonal freeze–thaw cycle: a 2-year comparative study between layered and homogeneous field soil profiles. J. Hydrol. 519, 1466–1473.
Gouttevin, I., et al., 2012. How the insulating properties of snow affect soil carbon distribution in the continental pan-Arctic area. J. Geophys. Res. Biogeosci. 117 (G2) n/a-n/a.
Grillakis, M.G., Koutroulis, A.G., Papadimitriou, L.V., Daliakopoulos, I.N., Tsanis, I.K., 2016. Climate-induced shifts in global soil temperature regimes. Soil Sci. 181 (6), 264–272.
Guo, D., Wang, H., 2014. Simulated change in the near-surface soil freeze/thaw cycle on the Tibetan Plateau from 1981 to 2010. Chin. Sci. Bull. 59 (20), 2439–2448.
Guo, D., Wang, H., 2016. CMIP5 permafrost degradation projection:a comparison among different regions. J. Geophys. Res. Atmos. 121 (9), 4499–4517.
Gutiérrez-Jurado, H.A., et al., 2013. On the observed ecohydrologic dynamics of a semiarid basin with aspect-delimited ecosystems. Water Resour. Res. 49 (12), 8263–8284.
Hagedorn, F., et al., 2014. Treeline advances along the Urals mountain range - driven by improved winter conditions? Global Change Biol. 20 (11), 3530–3543.
Hais, M., Chytrý, M., Horsák, M., 2016. Exposure-related forest-steppe: a diverse landscape type determined by topography and climate. J. Arid. Environ. 135, 75–84.
Han, L., Tsunekawa, A., Tsubo, M., 2010. Monitoring near-surface soil freeze–thaw cycles in northern China and Mongolia from 1998 to 2007. Int. J. Appl. Earth Obs. Geoinf. 12 (5), 375–384.
Henry, H.A.L., 2007. Soil freeze–thaw cycle experiments: trends, methodological weaknesses and suggested improvements. Soil Biol. Biochem. 39 (5), 977–986.
Hodgkins, S.B., et al., 2014. Changes in peat chemistry associated with permafrost thaw increase greenhouse gas production. Proc. Natl. Acad. Sci. U. S. A. 111 (16), 5819–5824.
Hollesen, J., Matthiesen, H., Møller, A.B., Elberling, B., 2015. Permafrost thawing in organic Arctic soils accelerated by ground heat production. Nat. Clim. Change 5 (6), 574–578.
Hu, G., et al., 2013. Forest buffers soil temperature and postpones soil thaw as indicated by a three-year large-scale soil temperature monitoring in the forest-steppe ecotone in inner Asia. Global Planet. Change 104, 1–6.
IPCC, 2013. Climate Change 2013 – The Physical Science Basis: Working Group I Contribution to the Fifth Assessment Report of the Intergovernmental Panel on Climate Change. Cambridge University Press, Cambridge.
Iwata, Y., Hayashi, M., Suzuki, S., Hirota, T., Hasegawa, S., 2010. Effects of snow cover on soil freezing, water movement, and snowmelt infiltration: a paired plot experiment. Water Resour. Res. 46 (9) n/a-n/a.
Jorgenson, M.T., et al., 2010. resilience and vulnerability of permafrost to climate change this article is one of a selection of papers from the dynamics of change in Alaska's boreal forests: resilience and vulnerability in response to climate warming. Can. J. For. Res. 40 (7), 1219–1236.
Kim, Y., Kimball, J.S., Didan, K., Henebry, G.M., 2014. Response of vegetation growth and productivity to spring climate indicators in the conterminous United States derived from satellite remote sensing data fusion. Agric. Forest Meteorol. 194, 132–143.
Knutti, R., Sedláček, J., 2012. Robustness and uncertainties in the new CMIP5 climate model projections. Nat. Clim. Change 3 (4), 369–373.
Kochy, M., Wilson, S.D., 1997. Litter decomposition and nitrogen dynamics in aspen forest and mixed-grass prairie. Ecology 78 (3), 732–739.
Koven, C.D., et al., 2011. Permafrost carbon-climate feedbacks accelerate global warming. Proc. Natl. Acad. Sci. U. S. A. 108 (36), 14769–14774.
Lawrence, D.M., Slater, A.G., Swenson, S.C., 2012. Simulation of present-day and future permafrost and seasonally frozen ground conditions in ccsm4. J. Clim. 25 (7), 2207–2225.
Lawrimore, J.H., et al., 2011. An overview of the global historical climatology network monthly mean temperature data set, version 3. J. Geophys. Res. (D19), 116.
Li, X., Jin, R., Pan, X., Zhang, T., Guo, J., 2012. Changes in the near-surface soil freeze–thaw cycle on the qinghai-tibetan plateau. Int. J. Appl. Earth Observ. Geoinf. 17, 33–42.
Lundberg, A., Nakai, Y., Thunehed, H., Halldin, S., 2004. Snow accumulation in forests from ground and remote-sensing data. Hydrol. Process. 18 (10), 1941–1955.
Luo, D., et al., 2016. Recent changes in the active layer thickness across the northern hemisphere. Environ. Earth Sci. (7), 75.
Namzalov, B.B., et al., 2012. Features of structure in zonal forest-steppe ecotone of South Siberia and Central Asia. Arid Ecosyst. 2 (2), 78–85.
Nelson, A.S., et al., 2016. Light absorption and light-use efficiency of juvenile white spruce trees in natural stands and plantations. For. Ecol. Manage. 376, 158–165.
Nelson, F.E., Outcalt, S.I., 1987. A computational method for prediction and regionalization of permafrost. Arct. Alp. Res. 19 (3), 279–288.
Park, H., Fedorov, A.N., Zheleznyak, M.N., Konstantinov, P.Y., Walsh, J.E., 2014a. Effect of snow cover on pan-arctic permafrost thermal regimes. Clim. Dyn. 44 (9-10), 2873–2895.
Park, H., Sherstiukov, A.B., Fedorov, A.N., Polyakov, I.V., Walsh, J.E., 2014b. An observation-based assessment of the influences of air temperature and snow depth on soil temperature in Russia. Environ. Res. Lett. 9 (6), 064026.
Peng, X., et al., 2017. Response of seasonal soil freeze depth to climate change across China. Cryosphere 11 (3), 1059–1073.
Pomeroy, J.W., Gray, D.M., Hedstrom, N.R., Janowicz, J.R., 2002. Prediction of seasonal snow accumulation in cold climate forests. Hydrol. Process. 16 (18), 3543–3558.
Rasmus, S., Lundell, R., Saarinen, T., 2011. Interactions between snow, canopy, and vegetation in a boreal coniferous forest. Plant Ecol. Divers. 4 (1), 55–65.
Schindlbacher, A., Jandl, R., Schindlbacher, S., 2014. Natural variations in snow cover do not affect the annual soil CO2 efflux from a mid-elevation temperate forest. Global Change Biol. 20 (2), 622–632.
Schuur, E.A., et al., 2015. Climate change and the permafrost carbon feedback. Nature 520 (7546), 171–179.
Slater, A.G., Lawrence, D.M., 2013. Diagnosing present and future permafrost from climate models. J. Clim. 26 (15), 5608–5623.
Smolander, S., Stenberg, P., 2001. A method for estimating light interception by a conifer shoot. Tree Physiol. 21 (12-13), 797–803.
Sun, Y., et al., 2012. Determining in-situ soil freeze–thaw cycle dynamics using an access tube-based dielectric sensor. Geoderma 189–190, 321–327.
Tarnocai, C., et al., 2009. Soil organic carbon pools in the northern circumpolar permafrost region. Global Biogeochem. Cycles 23 (2) n/a-n/a.
Wang, C., et al., 2013. Seasonality of soil CO2 efflux in a temperate forest: biophysical effects of snowpack and spring freeze–thaw cycles. Agric. For. Meteorol. 177, 83–92.
Wang, W., et al., 2016. Evaluation of air–soil temperature relationships simulated by land surface models during winter across the permafrost region. Cryosphere 10 (4), 1721–1737.
Wu, Q., Hou, Y., Yun, H., Liu, Y., 2015. Changes in active-layer thickness and near-surface

permafrost between 2002 and 2012 in alpine ecosystems, Qinghai–Xizang (Tibet) Plateau, China. Global Planet Change 124, 149–155.
Wu, X., et al., 2016. Seasonal divergence in the interannual responses of Northern Hemisphere vegetation activity to variations in diurnal climate. Sci. Rep. 6, 19000.
Zhang, T., 2003. Investigation of the near-surface soil freeze-thaw cycle in the contiguous united states: algorithm development and validation. J. Geophys. Res. 108 (D22).
Zhang, T., 2005. Spatial and temporal variability in active layer thickness over the Russian Arctic drainage basin. J. Geophys. Res. (D16), 110.
Zhang, T., Barry, R.G., Knowles, K., Heginbottom, J.A., Brown, J., 1999. Statistics and characteristics of permafrost and ground-ice distribution in the Northern Hemisphere1. Polar Geog. 23 (2), 132–154.
Zimov, S.A., Schuur, E.A.G., Chapin, F.S., 2006. Permafrost and the global carbon budget. Science 312 (5780), 1612–1613.